

New Launch Methodologies for the Micro-Millennia

Chrishma Hunter Singh-Derewa et al.

STARHUNTER CORPORATION
P.O. Box 941085
Maitland, Florida 32794
United States of America
321-356-STAR

Abstract: Rapid advancements in nano-technology have led to numerous improvements in microsatellite design. In the past twenty years, this class of satellites (10-100 kg mass) has repeatedly demonstrated their worth as vehicles for space science, technology demonstration, communications, remote sensing, education and information transfer. Within the past decade, the dramatic transition from experimentation to significant applications has prompted the implementation of numerous new launch methodologies. However, none have adequately met all the requirements stipulated by the small satellite market. The STARSAT launch vehicle has been tailored to specifically address the needs of the micro-satellite mission at a fraction of the cost of conventional launch systems. In addition, the predefined orbital parameters of these historically secondary payloads are no longer adequate for these mature and significant satellite missions. The implementation of the STARSAT design will enable low earth orbital insertion at any inclination without a corresponding increase in consumer cost. STARSAT will permit a wide array of scientific organizations, engineering corporations, universities, and even individuals, economically realistic access to space.

The STARSAT launch system utilizes high altitude space balloons coupled with an optimized propulsion platform to initiate a high performance LEO (Low Earth Orbit) transfer maneuver from a stratospheric altitude of 20 to 25 kilometers. Lack of drag, near earth gravity, and high atmospheric pressures coupled with a heavy focus on reducing overall payload mass enables STARSAT to achieve high orbital altitudes with minimal propulsion requirements. Phase 1 of the STARSAT design, fabrication and launch underway at the Kennedy Space Center in Florida is led by the development teams of STARHUNTER Corporation in conjunction with the National Aeronautics and Space Administration, The Florida Space Institute and the Central Florida Remote Sensing Labs.

This conceptual report details the STARSAT orbital insertion profile, as well as subsystem design with a focus on propulsion and guidance techniques. Telemetry from the maiden launch of STARSAT will be discussed, in addition to future design goals. Overall, STARSAT has resulted in a cost effective mission profile for use throughout the small satellite industry.

Introduction

The STARSAT launch platform has been optimized to deliver micro-satellites to low earth orbit for a fraction of the cost of conventional launch systems while maximizing environmental, safety and reliability. Reliable solid motor thruster technology coupled with commercial subsystem nano-technology enables this passive first stage to orbit design to perform Hohmann transfer insertion with relative ease. A low cost test was executed at the Kennedy Space Center to assure mission success including:

- Payload interface compatibility
- Systems end-to-end operability and functionality
- Utilization of real time telemetry
- Data analysis of stratospheric environmental effects

Implementing a low cost launch system with minimal environmental impact will revolutionize the small satellite market. STARHUNTER Corporations' STARSAT System satisfies the needs of this ever-expanding market by providing economical launch opportunities for small payloads.

STARSAT Organization

Responding to a NASA directive: “launch 12 small payloads per year with an increase within 3 years to 24 per year” STARHUNTER Corporation has designed and developed an innovative launch design utilizing stratospheric space balloons. STARHUNTER Corporation has contracted with the Florida Space Institute, the University of Central Florida and NASA to design a small satellite payload and the means of delivering it to low earth orbit.

STARHUNTER Corporation defined mission objectives using consumer-defined parameters. While focusing on consumer need, the team also addresses political and legal obstacles, isolates available resources, and defines economic constraints. STARHUNTER Corporation seeks to reduce processing requirements and vehicle turn around time while facilitating orbital insertion by allowing customers to define STARSAT requirements.

Capitalizing on an initial altitude of 25 kilometers, the STARSAT system exponentially reduces the propellant requirements seen by conventional methods. STARSAT subsystem design employs “nano-sat” flight hardware selected to further reduce propellant requirements. An in depth review of the environmental effects on a stratospheric launch platform. These studies have permitted the engineering team to further maximize the STARSAT thrust profile by improving nozzle performance and aerodynamic design.

STARSAT Development

Despite the emergence of numerous alternative launch designs, such as; Johns Hopkins Applied Physics Laboratory’s Light Gas Gun; EUROCKOTs’ Rockot Launch System; Orbitals’ air launched Pegasus rocket and ground-launched Taurus and Minotaur lift vehicles, using surplus ICBM missiles; in addition to Boeings’ Sea Launch platform the Small Satellite community is still seeking a complete solution to their launch requirements. Thus far the answers have not adequately met the economic constraints of the typical small satellite mission.

Processing complexity, manpower demands and high fuel requirements kept these launch vehicles large and costly. The typical launch costs a small satellite designer might encounter is still quite commonly in the million-dollar range, typically the budget of the micro-sat itself.

The STARSAT launch system is many times cheaper than many of its competitors tailoring its system to ultra light missions. Utilizing COTS (Commercial Off The Shelf) hardware while focusing on a creative yet cost conscious engineering environment has allowed the cost of a STARSAT launch to remain under ten thousand dollars.

Subsystem	Cost	Margin	Cost with Margin
STARSAT SYSTEMS BUDGET			
Propulsion	1000	25%	1,250
Communications	1,000	25%	1,250
C&DH	200	25%	250
Power	250	25%	310
ADCS	240	25%	300
Thermal	25	25%	32
Structure	1,000	25%	1,250
Total	3,715		4,642

Table 1.1: STARSAT Systems Budget

The total cost of the STARSAT launch vehicle, including a 25% design margin, totals 4,642 dollars as seen in table 1.1 above. This budget assumes a low earth orbital insertion with standardized telemetry requirements.

Advancements in subsystem electronics and structural materials, as well as commercialization of previously specialized components allow engineers increased selection flexibility at a fraction of historical prices. Composite materials, battery life, and cellular technologies are among the advancements that have helped minimize the overall cost of a STARSAT launch without sacrificing quality and reliability.

Other technological contributions to the STARSAT design include the use of the military’s Global Positioning System. The GPS unit aboard STARSAT acts as both an altimeter and as a navigation unit. During the technology demonstration phase, engineers rely on GPS to validate the altitude achieved. The Command and Data Handling system takes advantage of increased processing performance and low hardware prices for onboard computing. Structural subsystems benefit from advances in carbon-carbon composites and polyurethane foam, detailed in the engineering design section.

In addition to the accessibility of needed technology, STARSAT also arose from specific technological demands. The Hitchhiker Ejection System follows a predetermined orbital profile that ejects the accompanying satellite during its defined shuttle mission parameters. With the next 20 years dedicated almost entirely to the assembly of the International Space Station at 56 degrees latitude, the chance of a piggyback mission attaining its' required orbital inclination is greatly reduced. Secondly, the reliability of the new generation of smaller rockets is questionable. Currently experiencing almost a 50% failure rate, the need for a new launch system emphasizing reliability as well as cost savings was even more necessary.

The requirements for the STARSAT launch system are simple focusing on minimal mass and maximum altitude as shown in table

Payload	Minimize payload mass Maximize altitude achieved
Guidance	$\pm 5^\circ$ nadir attitude control Yaw control during ascent
Communication	2 way at elevation >20 km
Telemetry	Commands - 7K bps Science data - 8K bps active mode (1MB / 5min) Health - 36 hour history, 64 ch, 8 bits, 1 sample/min
Orbit	Inclination defined by customer at a 94 km altitude
Lifetime	1 day
STARSAT constraints	Max 66 lbs (30 kg) Max 30" dia, 40" height Max c.m. 10.5" axial, 0.5" radial

Table 1.2 – Requirements and Constraints

STARSAT DESIGN

1. Orbital Dynamics

It has been assumed that an orbital maneuver will lift the vehicle from an initial launch altitude of 20km to a final insertion altitude of 94000m. At this minimum altitude the satellite will remain in orbit approximately 1 to 2 days. Phase One of the STARSAT development concept is to attain the minimum altitude defined as Space; an altitude where an object in orbit will remain in orbit briefly (only a day or two in some cases) before air molecules in the atmosphere drag it back to earth. Since the assumption has been made that this experiment is simply a change of orbits, there will be no escape velocity calculations.

Once the STARSAT system has delivered the payload to stratospheric altitude, thrusters are activated initiating a Hohmann transfer orbital maneuver. By using the Earth's gravity as a slingshot to swing the payload around to a higher apogee and at that apogee perform a Hohmann transfer, which is a burn to change from one type of orbit to another, STARSAT places a payload into low-Earth orbit using less propellant than is conventionally necessary.

The procedure in the analytical solution is as follows: A transfer orbit connects orbit 1 to orbit. To get from orbit 1 to the transfer orbit, there is need to change the energy (\approx). Then, when the transfer orbit reaches the altitude of orbit 2, the energy has to be changed again. As a result, the complete maneuver that will take the object from orbit 1 to orbit 2 requires two separate velocity changes (ΔV_1 and ΔV_2). If a ΔV_2 is *not* performed the object will remain in the transfer orbit and return to perigee where the launch took place. During Phase One of STARSAT development only the transfer orbit will be attempted to prove feasibility.

Analytical Solution

- 1) Compute semi-major axis (
- a_{transfer}
-) of transfer orbit

$$R_{\text{orbit1}} = (a_{\text{orbit1}}) = 6378140 \text{ m} + 20000 \text{ m}$$

$$(a_{\text{orbit1}}) = \mathbf{6398140 \text{ m}}$$

$$R_{\text{orbit2}} = (a_{\text{orbit2}}) = 6378140 \text{ m} + 94000 \text{ m}$$

$$(a_{\text{orbit2}}) = \mathbf{6472140 \text{ m}}$$

$$a_{\text{transfer}} = (R_{\text{orbit1}} + R_{\text{orbit2}}) / 2$$

$$a_{\text{transfer}} = (6398140 \text{ m} + 6472140 \text{ m}) / 2$$

$$a_{\text{transfer}} = \mathbf{6435140 \text{ m}}$$

- 2) Solution for the specific mechanical energy (
- $\epsilon_{\text{transfer}}$
-) of the transfer orbit.

$$\mathbb{G} = 3.986 \text{E}14 \text{ m}^3/\text{s}^2$$

(gravitational parameter)

$$\epsilon_{\text{transfer}} = - (\mathbb{G} / 2 a_{\text{transfer}})$$

$$= - [(3.986 \text{E}14 \text{ m}^3/\text{s}^2) / 2(6435140 \text{ m})]$$

$$\epsilon_{\text{transfer}} = \mathbf{-3.097 \text{E}7 \text{ m}^2/\text{s}^2}$$

(Energy is negative, which implies the transfer orbit is an ellipse as expected.)

- 3) Solution for energy (
- ϵ_{orbit1}
-) and velocity (
- V_{orbit1}
-) of orbit 1.

$$\epsilon_{\text{orbit1}} = - (\mathbb{G} / 2 a_{\text{orbit1}})$$

$$= (3.986 \text{E}14 \text{ m}^3/\text{s}^2) / 2(6398140 \text{ m})$$

$$\epsilon_{\text{orbit1}} = \mathbf{-3.115 \text{E}7 \text{ m}^2/\text{s}^2}$$

$$V_{\text{orbit1}} = \{2 [(\mathbb{G} / R_{\text{orbit1}}) + \epsilon_{\text{orbit1}}] \}^{1/2}$$

$$V_{\text{orbit1}} = \{2 [(3.986 \text{E}14 \text{ m}^3/\text{s}^2 / 6398140 \text{ m}) - 3.115 \text{E}7 \text{ m}^2/\text{s}^2] \}^{1/2}$$

$$= \{2 [(3.115 \text{E}7 \text{ m}^2/\text{s}^2)] \}^{1/2}$$

$$V_{\text{orbit1}} = \mathbf{7893.03 \text{ m/s}}$$

- 4) Solution for
- V_{transfer}
- at orbit
- ₁

$$V_{\text{transfer}} \text{ at orbit}_1 = \{2 [(\mathbb{G} / R_{\text{orbit1}}) + \epsilon_{\text{transfer}}] \}^{1/2}$$

$$V_{\text{transfer}} \text{ at orbit}_1 = \{2 [(3.986 \text{E}14 \text{ m}^3/\text{s}^2 / 6398140 \text{ m}) - 3.097 \text{E}7 \text{ m}^2/\text{s}^2] \}^{1/2}$$

$$V_{\text{transfer}} \text{ at orbit}_1 = \{2 [(3.133 \text{E}7 \text{ m}^2/\text{s}^2)] \}^{1/2}$$

$$V_{\text{transfer}} \text{ at orbit}_1 = \mathbf{7915.73 \text{ m/s}}$$

- 5) Find
- ΔV_1

$$\Delta V_1 = | V_{\text{transfer}} \text{ at orbit}_1 - V_{\text{orbit1}} |$$

$$= | 7915.73 \text{ m/s} - 7893.03 \text{ m/s} |$$

$$\Delta V_1 = \mathbf{22.7 \text{ m/s}}$$

- 6) Solution for
- V_{transfer}
- at orbit
- ₂

$$V_{\text{transfer}} \text{ at orbit}_2 = \{2 [(\mathbb{G} / R_{\text{orbit2}}) + \epsilon_{\text{transfer}}] \}^{1/2}$$

$$V_{\text{transfer}} \text{ at orbit}_2 = \{2 [(3.986 \text{E}14 \text{ m}^3/\text{s}^2 / 6472140 \text{ m}) - 3.097 \text{E}7 \text{ m}^2/\text{s}^2] \}^{1/2}$$

$$V_{\text{transfer}} \text{ at orbit}_2 = \{2 [(3.062 \text{E}7 \text{ m}^2/\text{s}^2)] \}^{1/2}$$

$$V_{\text{transfer}} \text{ at orbit}_2 = \mathbf{7825.22 \text{ m/s}}$$

- 7) Solution for energy (
- ϵ_{orbit2}
-) and velocity (
- V_{orbit2}
-) in orbit 2.

$$\epsilon_{\text{orbit2}} = - (\mathbb{G} / 2 a_{\text{orbit2}})$$

$$= [(3.986 \text{E}14 \text{ m}^3/\text{s}^2) / 2(6472140 \text{ m})]$$

$$\epsilon_{\text{orbit2}} = \mathbf{-3.079 \text{E}7 \text{ m}^2/\text{s}^2}$$

$$V_{\text{orbit2}} = \{2 [(\mathbb{G} / R_{\text{orbit2}}) + \epsilon_{\text{orbit2}}] \}^{1/2}$$

$$V_{\text{orbit2}} = \{2 [(3.986 \text{E}14 \text{ m}^3/\text{s}^2 / 6472140 \text{ m}) - 3.079 \text{E}7 \text{ m}^2/\text{s}^2] \}^{1/2}$$

$$V_{\text{orbit2}} = \{2 [(3.079 \text{E}7 \text{ m}^2/\text{s}^2)] \}^{1/2}$$

$$V_{\text{orbit2}} = \mathbf{7848.19 \text{ m/s}}$$

- 8) Find
- ΔV_2

$$\Delta V_2 = | V_{\text{orbit2}} - V_{\text{transfer}} \text{ at orbit}_2 |$$

$$\Delta V_2 = \mathbf{22.7 \text{ m/s}}$$

2. Structural Design and Analysis

Support of the satellite's payload, subsystems, and the Space Balloon clamp interface are provided by the STARSAT bus structure. To survive ground handling, launch, and mission environments, the strength, stiffness, and thermal properties of the structure must be carefully selected. The design approach used for the STARSAT structure subsystem is based on that described in *Spacecraft Structures and Mechanisms* [3]. The mission, payload, orbit, and launch vehicle requirements are first defined. Configuration design follows, including an iteration of subsystem concepts, structural architecture, and component layouts. At the end of each design iteration the system is analyzed to verify compliance with the requirements.

2.1 Requirements

Minimizing subsystem weight and withstanding the expected loads are the primary structural requirements for STARSAT. The launch loading conditions are the most severe, and therefore drive the design.

The current lift capacity of the STARSAT space balloon system is approximately 14 kg, half of which is reserved for propellant. The remaining 7 kg must incorporate structure and individual subsystems.

2.2 Configuration Design

The structure itself will be composed of a PVC cylindrical casing. This fairing, with attached rocket motor and nozzle, will rest within an adjustable guide tube. The total estimated mass of this structure is 4 kg. As illustrated in figure 2.1 the satellite electronics and sensors will be encased within the rocket nose cone fairing. The space between the payload and the fairing will be filled with expandable polyurethane foam to provide additional insulation and help prevent possible vibration damage.

To facilitate assembly and access, STARSAT uses a modular design with three sections defined by component mounting plates. The payload sensors make up the first module. Command and data handling (C&DH) and communications components, including the ignition circuitry, are in the second; module three contains Attitude determination and control (ADCS) and the power system components.

The rocket will rest within the guide tube, secured by protruding support nodes located above the center of gravity. Sensors such as humidity, pressure, temperature and communications antennae, will extend outward through guide channels in the guide tube. This configuration, which can be seen in figure 2.2, ensures minimal interference for ground-to-air radio communication.

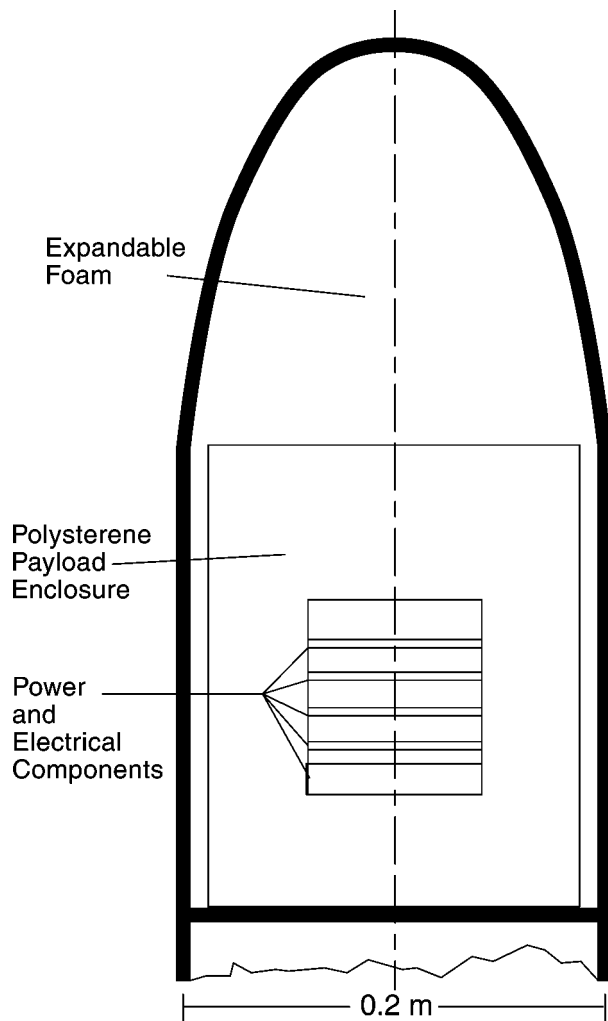


Figure 2.1: Payload Enclosure

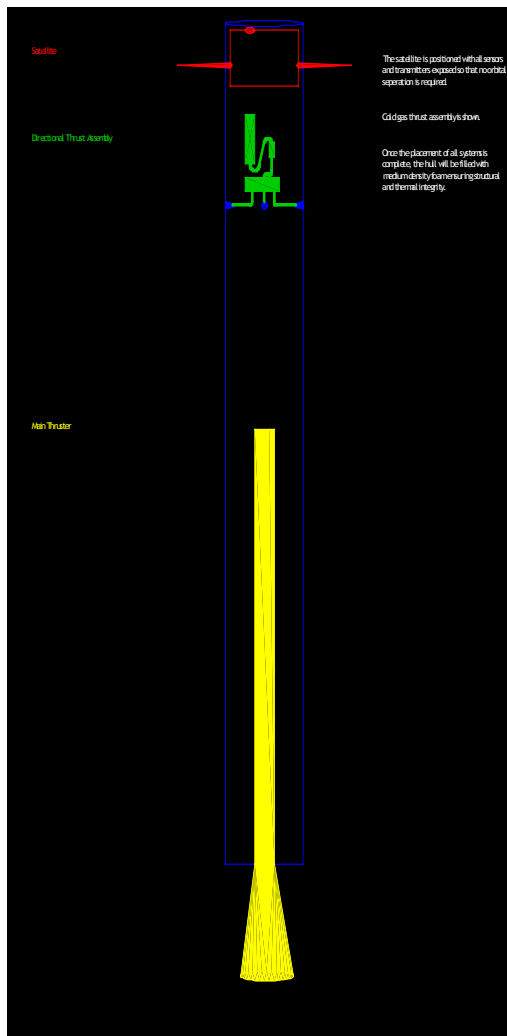


Figure 2.2: Stowed Configuration

2.3 Balloon Design

The next important step in the structural design is the selection of the size and type of balloon to be used, and a determination of which lifting gas will be utilized. Due to its volatile nature, hydrogen will not be used. Nitrogen has a greater lifting capacity than helium, nitrogen will be the lifting agent in the balloon. The balloon must be large enough to hold the amount of nitrogen gas required to lift the rocket assembly. It must also be able to expand, as the ambient air pressure will decrease as the balloon's altitude increases. The optimal type of material to use for the lifting balloon is natural rubber, as it has the greatest capacity to expand for its size and weight. The type of balloon that we found to best meet our requirements is the KCI 3000 made by Totex. The number of balloons to be used will be

determined by the final weight of the entire launch system and payload. Table 4.1 details the size, maximum altitude before bursting, and the amount of nitrogen gas required to lift a 6 kg payload at a rate of 320 meters per minute to an altitude of 37.9 km.

Specifications for KCI TX1200

Average Weight	3 kg
Diameter Before Inflation	227 cm
Diameter At Release	212 cm
Maximum Altitude	37.9 km
Required Gas to Lift 1.05 kg Payload	4.97 m ³

Table 4.1 : Totex Balloon Specifications

During any one of the launch phases, something could go wrong that places the mission in jeopardy. The primary concern is the module falling back to Earth and causing damage, should the balloon become punctured or the solid motor fail to fire during phase two. To prevent this from occurring, rather than using redundant thrusters on the system, a small parachute will be attached to the launch tube. This encased parachute takes up only eight cubic inches, and once deployed, unfurls to a radius of two feet. The parachute is also aligned in such a manner as to prevent alignment of the mercury switches discussed later at any time.

3. Propulsion

STARHUNTER's propulsion system consists of a primary motor for boosting the spacecraft to its desired altitude, and a series of microthrusters for attitude control. The attitude control thrusters are discussed in the next section. For the primary motor, there are several different types of propulsion technologies to be considered: cold gas, solid, liquid monopropellant, liquid bipropellant, liquid dual mode, liquid hybrid, and electric. Two factors that must be considered are the impact that the propellant will have on the environment, and which propellant will give the highest thrust-to-propellant ratio. The second factor eliminates cold gas, electric, monopropellant, and dual mode propulsion systems. This leaves solid propellants, liquid bipropellants, and hybrid propellants. While each propellant is efficient and has the ability to produce a relatively large amount of thrust, each has its drawbacks. Table 3.1 below lists the types of propellants that are being considered, their performances, and the advantages and disadvantages of each.

Performance and Characteristics of Propellants

Type	Propellant	Thrust Range	Advantages	Disadvantages
Solid Motor		50-5x10 ⁶	Simple, reliable, relatively low cost	Limited Performance, Lower Thrust, Safety Issues, Performance Not Adjustable
Liquid Bipropellant	O ₂ and RP-1	5-5x10 ⁶	High Performance	More Complicated System
	N ₂ O ₄ and MMH	5-5x10 ⁶	Storable, Good Performance	Complicated System
	F ₂ and N ₂ H ₄	5-5x10 ⁶	Very High Performance	Toxic, Dangerous, Complicated
	OF ₂ and B ₂ H ₆	5-5x10 ⁶	Very High Performance	Toxic, Dangerous, Complicated
	ClF ₃ and N ₂ H ₄	5-5x10 ⁶	High Performance	Toxic, Dangerous
Hybrid Motor	HTPB and IRFNA	225-3.5x10 ⁵	Throttleable, Nonexplosive, Nontoxic, Restartable	Requires Oxidizer, Bulkier Than Solids

Table 3.1 : Propulsion Comparison

The propulsion engineering team determined that the type of motor best suited to STARSAT's mission parameters is an Aerotek K240 solid rocket motor carrying 1.2 kilograms of fuel. This motor is both highly cost-efficient and light. Since solid propellants cannot be shut off once they are ignited, multiple microthrusters are utilized to affect attitude control.

4. Attitude Control and Determination

Micro-Electromechanical Systems (MEMS) thrusters (as seen in figure 6.1) designed by NASA will perform navigational adjustments in the case of a course change or correction. MEMS are a new type of thruster that uses small amounts of propellant to burn at a controlled rate. They are extremely small and compact. With this newly developed type of thruster, the three components necessary to reach the desired altitude have been defined: a balloon to raise the unit into the upper atmosphere, a solid rocket to lift the satellite the remaining 80 kilometers, and MEMS thrusters that will perform attitude adjustments. In future phases of the STARSAT project, an additional propulsion system, such as a hybrid motor, will be required for orbital insertion when the spacecraft reaches its apogee.

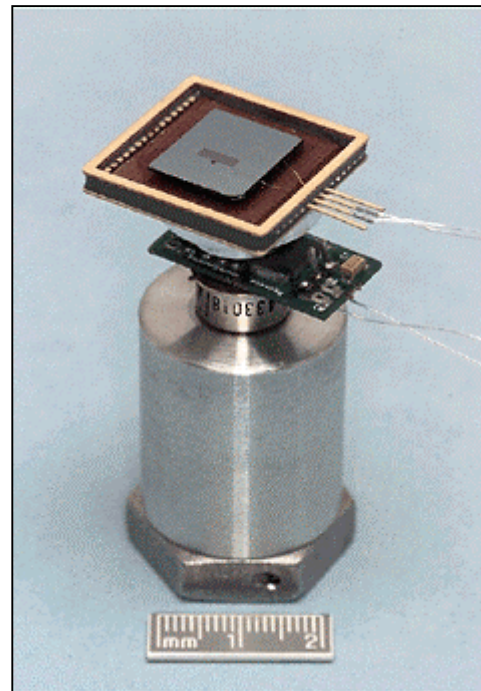


Figure 4.1: Conventional MEMS Thruster

4.1 Requirements and Major Functions

As discussed in the previous section, MEMS thruster technology is utilized to adjust the attitude of the STARSAT system during ascension. MEMS work by using a very small amount of propellant to adjust a missile's trajectory. They are more efficient than conventional propulsion systems for three reasons: 1) they have a much smaller mass than conventional systems; 2) they have a thrust-to-weight ratio greater than one; and 3) because the shape of their nozzles can be easily changed, they are able to be optimized for whatever altitude they will operate.

4.2 ACS Configuration

With an understanding of the MEMS thruster and how it works, the next step is to select the type of propellant to be utilized. A new type of MEMS thruster is being developed by NASA's Jet Propulsion Laboratory, which uses a miniature heating pad to vaporize water as it passes through the combustion chamber, thus forcing steam out the nozzle at a high velocity. Not only is this a more simple method than both the liquid and hybrid systems, it requires relatively little space for storing the water. Since the flow rate can be controlled, the thrust can be controlled. A water vaporization thruster does not combust; it can be turned on and off at will; and most importantly, is 100 percent environmentally friendly. A schematic of the selected water vaporization system this system is seen below in figure 4.2.

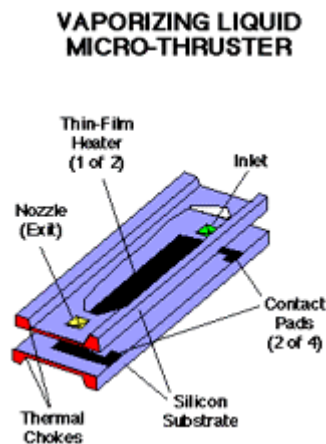


Figure 4.2 :
Vaporizing MEMS Thruster

4.2 ADS Configuration

During ascent it is crucial that STARSAT be able to accurately sense its altitude and orientation. Positional data will be determined using a GPS receiver and a piezoelectric gyroscope to initiate corrective measures using the MEMS thrusters, as well as validate achieved attitude.

The GPS receiver will send its data to a packet controller and transmitter. This will report balloon latitude, longitude and altitude. The Global Positioning System (GPS) is a worldwide radio-navigation system formed from a constellation of 24 satellites and their ground stations.

GPS uses these "man-made stars" as reference points to calculate positions accurate to a matter of meters. Due to government regulations, many GPS receivers will not function above 60,000 feet, which is a potential problem. Export regulations were designed to prevent foreign governments from improving the accuracy of their missiles. The actual regulations ban export of GPS receivers that can measure speeds in excess of several hundred miles per hour at altitudes above 60,000 feet. Motorola GPS boards are reputed to work above 60,000 feet at typical balloon speeds and will be used aboard STARSAT. A special version of their firmware will be utilized that will deliver data above 60,000 feet. A non-export agreement has been initiated to attain this software. The accuracy of GPS signals is also intentionally degraded to about 100 yards horizontally and 300-500 feet vertically, again to restrict the accuracy of potential aggressors.

The Motorola GPS receiver has a 4800 baud RS-232 ASCII output in a standardized format. It was originally designed for use on boats, to allow LORAN receivers to work with autopilots. The GPS receiver is programmed to send latitude, longitude and altitude continuously.

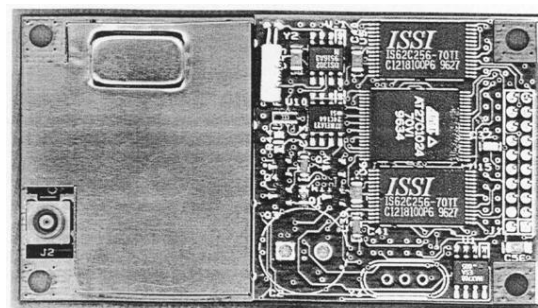


Figure 4.3: The Rockwell "Jupiter" GPS Receiver

The attitude determination and control of the spacecraft will be achieved using a position-plus-rate feedback control system for the pitch, roll and yaw axes. A general block diagram of the ADCS is shown below in Figure 4.5. Although the primary stabilization is passive, control is required for initial orientation, payload orientation, and damping.

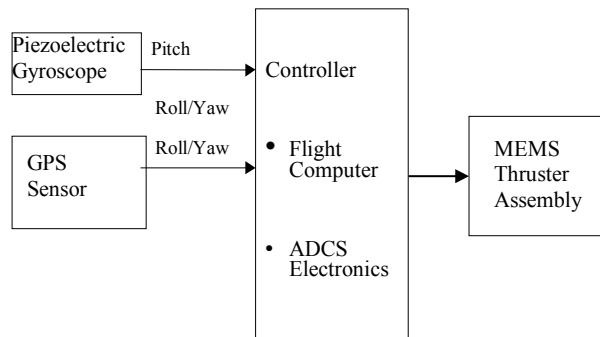


Figure 4.4: ADCS Control Block Diagram

The attitude determination system will provide the necessary information to verify correct orientation as well as to update the control system. Piezoelectric gyroscopes similar to the ones used on model airplanes will be used to sense rocket orientation.



Figure 4.5: Hobbico Super Small Multi-Purpose Micro Piezoelectric Gyroscope

The multi-purpose piezoelectric gyro shown in Figure 4.5 is an exceptionally small, single-axis gyroscope. With dimensions of 1.1 x 1.1 x 0.6 inches and a weight of less than half an ounce, this gyroscope is ideal for use in a small satellite where additional weight is a critical factor. The fast response time of these gyros allows faster and therefore more accurate attitude adjustments from the MEMS thrusters.

5. Nozzle Optimization

The standard shape of a rocket motor's nozzle is the familiar bell shape. This shape works because the pressure of the atmosphere allows for the molecules coming out of the nozzle to push against something. In a low or zero pressure environment the most efficient

type of nozzle is a long narrow one. The highest thrust is obtained when the exit pressure equals the ambient pressure. The exit pressure is governed by the relationship between the nozzle exit area and the area of the throat of the nozzle. For an engine near the ground, where the ambient pressure is relatively high, a nozzle with a small area expansion ratio, ϵ (ratio of the nozzle exit area to the area of the throat), is usually desired. However, for an engine in the upper atmosphere approaching space, the ambient pressure is nearly zero. Therefore the more optimum nozzle is one with a very large expansion ratio.

Nozzles are designed to keep the exit pressure as close to the ambient pressure as possible. In space it is ideal to decrease the exit pressure as much as possible. Basically, thrust is provided by the difference between the pressure in the chamber and the exit pressure. The pressure is the lowest at the exit where the velocity is the highest. Since a nozzle is a type of diffuser, where velocity increases and pressure decreases as the area decreases, normal subsonic flow nozzles are in the shape of a cone. However, once velocities reach and exceed Mach 1 the flow properties change so that at supersonic flow the velocity increases (and pressure further decreases) as the area increases (the opposite effect). This is what gives the nozzle the hourglass shape. Ideally the velocity of the gases should reach Mach 1 at the throat (where the cross sectional area is the smallest). So at the exit of the nozzle, the area is the greatest, and the greater the area at the exit the higher the velocity and hence the lower the pressure. The exit pressure is controlled by this area ratio called the nozzle-area expansion ratio:

$$\epsilon = A_e / A_t$$

where A_e is the exit cross-sectional area and A_t is the area at the throat. Thus, in near-space conditions, increasing the area ratio increases the thrust. It is possible to increase this area until the added weight and internal drag losses of a longer nozzle costs more in performance than the thrust it creates.

Optimum area ratio can be determined for a specific altitude. Given that P_c (Combustion Chamber Pressure), and P_{atm} (Atmospheric Pressure), and A_t are known, the optimum area ratio can be determined assuming the exit pressure is equal to the atmospheric pressure using the following two equations. M_e is the Mach number and γ is fixed at 1.2 for gaseous oxygen/hydrogen mixtures.

$$M_e^2 = \frac{2}{(\gamma - 1)} * \left\{ \left(\frac{P_c}{P_{atm}} \right)^{\frac{(\gamma - 1)}{\gamma}} - 1 \right\}$$

$$\frac{A_e}{A_t} = \left(\frac{1}{M_e} \right) * \frac{\left\{ 1 + \frac{(\gamma - 1)}{2} * M_e^2 \right\}}{\left(\frac{\gamma + 1}{2} \right)^{\frac{(\gamma + 1)}{2(\gamma - 1)}}}$$

The optimum exit area at the altitudes of 20km and 100km were averaged to provide the peak optimization for the STARSAT system.

F

 V_e
 m

Governing Equation :

$$F = mV_e + A_e [P_e - P_\infty]$$

= The amount of force applied to the rocket based on the expulsion of gasses where:

A_e = The nozzle exit area

= The gas pressure at the nozzle exit

P_∞ = The ambient pressure

= The propellant exhaust velocity

= The propellant mass flow rate

The following tables illustrate the above relationships:

Examples of How Ambient Pressure Change Affects Force

$$F = mV_e + A_e [P_e - P_{amb}]$$

Altitude In Kilometers	Force In Newtons	Mass Flow Rate In kg/sec	Exhaust Velocity In m/s	Exhaust Area In m ²	Exhaust Pressure In millibars	Ambient Pressure In millibars
0	750	25	40	0.5	300	800
1	775	25	40	0.5	300	750
2	810	25	40	0.5	300	680
3	845	25	40	0.5	300	610
4	897.5	25	40	0.5	300	505
5	955	25	40	0.5	300	390
10	1070	25	40	0.5	300	270
15	1150	25	40	0.5	300	150
20	1230	25	40	0.5	300	70

Examples of How Change in Exhaust Area Affects Force

$$F = mV_e + A_e [P_e - P_{amb}]$$

Altitude In Kilometers	Force In Newtons	Mass Flow Rate In kg/sec	Exhaust Velocity In m/s	Exhaust Area In m ²	Exhaust Pressure In millibars	Ambient Pressure In millibars
20	1023	25	40	0.1	300	70
20	1046	25	40	0.2	300	70
20	1069	25	40	0.3	300	70
20	1092	25	40	0.4	300	70
20	1115	25	40	0.5	300	70
20	1138	25	40	0.6	300	70
20	1161	25	40	0.7	300	70
20	1184	25	40	0.8	300	70
20	1207	25	40	0.9	300	70

Table 5.1 : Effects of Pressure and Exit Area on Rocket Thrust

Since the optimum nozzle area ratio occurs at only one altitude, the nozzle with a fixed area ratio will mostly operate either overexpanded or underexpanded. An underexpanded nozzle is one where the exit pressure is greater than the ambient pressure. For an overexpanded nozzle, the exit pressure is less than the ambient pressure.

When selecting an expansion area ratio, the limiting factor is the thrust capability at the launch altitude (estimated at 20 km), and the increase in weight and drag as the nozzle increases in size. At the launch altitude (20 km) the nozzle will be overexpanded, i.e. $P_e < P_{atm}$. Focusing on the first criteria, the nozzle size cannot be too large where thrust is not achieved. For an overexpanded nozzle, the thrust decreases as the exit pressure becomes much less than the ambient pressure.

At roughly $P_e \leq 0.4 * P_{atm}$, flow separation occurs inside the nozzle. For a typical conical-shaped nozzle, separation is uniform and symmetric. However, during start and stop transients, the potential for non-symmetric separation and momentary flow oscillations to occur increases and may result in large side forces on the nozzle. These side forces during start-stop transients can potentially cause failure in the nozzle cone structure. The second criteria, increased drag and weight, play a big role in optimizing flight performance. However, this may be limited by the first criteria. Table 5.2 below summarizes various nozzle configurations and evaluations of the thrust coefficient over a range of altitudes. C_f , D_t , and D_e represent the thrust coefficient, diameter of the throat, and exit diameter, respectively.

Given:

$$P_c = 1200 \text{ psi}$$

$$k = 1.2$$

$$D_t = 0.228 \text{ inches}$$

Case A, $\varepsilon = 98.72$, $D_e = 2.27$ inches

Altitude, km	20	20.53	40	60	80	100
C_f	1.89	1.89	1.95	1.95	1.95	1.95
P_e / P_{atm}	1.00	1.00	19.25	246.07	5330.45	133616.67
Optimum C_f	1.89	1.89	2.03	2.11	2.17	2.20

Case B, $\varepsilon = 205.83$, $D_e = 3.27$ inches

Altitude, km	20	26.84	40	60	80	100
C_f	1.86	1.94	1.99	2.00	2.00	2.00
P_e / P_{atm}	0.40	1.00	7.70	98.43	2132.18	53446.67
Optimum C_f	1.89	1.94	2.03	2.11	2.17	2.20

Case C, $\varepsilon = 527.92$, $D_e = 5.24$ inches

Altitude, km	20	34.87	40	60	80	100
C_f	1.69	2.00	2.02	2.04	2.04	2.04
P_e / P_{atm}	0.12	1.00	2.40	30.69	664.89	16666.67
Optimum C_f	1.89	2.00	2.03	2.11	2.17	2.20

Case D, $\varepsilon = 927.38$, $D_e = 6.94$ inches

Altitude, km	20	39.64	40	60	80	100
C_f	1.45	2.03	2.03	2.06	2.07	2.07
P_e / P_{atm}	0.06	1.00	1.20	15.35	332.45	8333.33
Optimum C_f	1.89	2.03	2.03	2.11	2.17	2.20

Table 7.2 Various Nozzle configurations

For this project, selection of the size was determined on the basis of maximizing thrust while minimizing potential side forces due to flow separation at 20 km. Case 'B' was optimized just for that purpose where $P_e = 0.4 * P_{atm}$, the point at which flow separation is just about to occur.

The optimum nozzle shape is the common bell shape or contour design. This is the most effective at minimizing drag. The bell shaped nozzle, which is equivalent to a 15° half-angle cone, is a typically efficient size factoring both reduced drag, size, and weight. Figure 5.1, below illustrates the shape design of the bell versus the conical. The dimensions of the conical nozzle fit the description of Case 'B' nozzle configuration as mentioned earlier. The dotted line in Figure 5.1 indicates where the nozzle of the supplied engine ends and where the add-on nozzle begins.

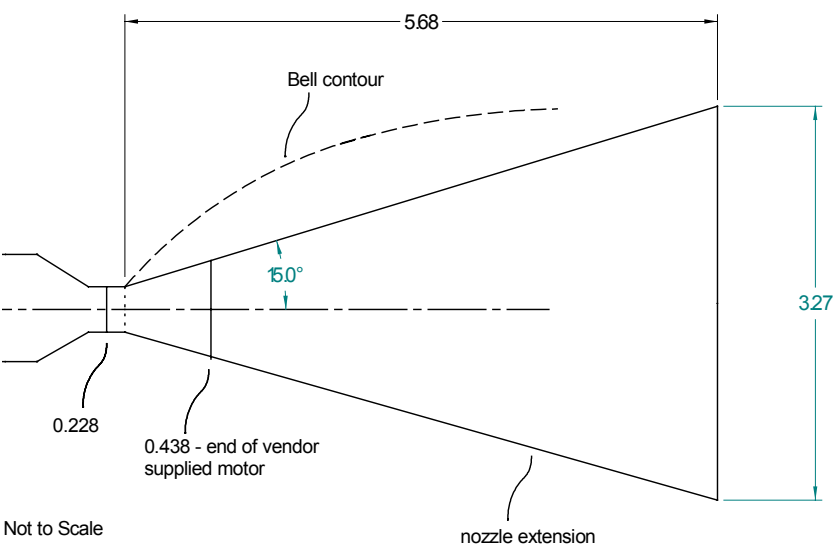


Figure 5.1: Case B Optimized Rocket Nozzle Config.

6. Thermal Control

The purpose of the thermal control subsystem is to maintain all mission-critical components within their operational temperature ranges. Conductive heat transfer from the rocket motor to the payload, as well as environmental factors are the primary concerns to be addressed by the thermal control design. These are the most likely factors to cause the payload components to exceed their range of thermal tolerances.

The STARSAT thermal design utilizes passive thermal control. This approach has the advantages of being simple, cost-effective, and demanding no additional power requirements. Passive thermal control is achieved by using thermal coatings and insulation materials, thermally isolating components from the environment, and specifying component interfaces.

6.1 Thermal Concerns and Environmental Factors

The first step in determining the thermal design is to establish both the operating and non-operating temperature ranges of the mission-critical components. These are given in Table 6.1. The component temperature ranges are then compared to the range of atmospheric temperatures expected to be encountered up to an altitude of 100 km.

Component	Non-Operating (°C)	Operating (°C)
Payload	-50/+80	-30/+60
Antenna	-170/+90	-170/+90
Receiver	-20/+70	0/+35
Transmitter	-40/+80	-30/+60
Battery	-10/+25	0/+25
Propulsion Assembly	-50/+80	-40/+40
MEMS Thrusters	-100/+85	-100/+85

Table 6.1 : Component Temperature Ranges

Figure 6.2 shows a plot of temperature vs. altitude. A comparison of these two data sets allows us to determine the maximum temperature difference between the upper and lower bounds of both temperature ranges. From this data we can estimate that the maximum temperature difference between the highest minimum component operating temperature and the lowest atmospheric temperature is approximately 91°C. This temperature difference will then dictate the required effectiveness of the thermal protection.

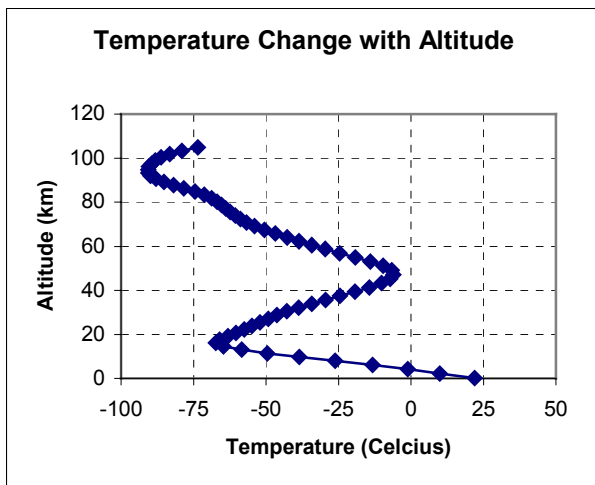


Figure 6.2 : Temperature vs. Altitude

As altitude increases, pressure decreases, which reduces the effects of heat transfer by convection. At the altitude where STARSAT will be exposed to the coldest temperatures, ambient pressure will be low enough to disregard convection as a significant contribution to heat loss of the spacecraft. The battery and electrical components will be contained within a modular polystyrene enclosure that will in turn be covered by an outer fairing. For this reason, the effects of heat transfer due to conduction will be considered.

The only notable factor capable of surpassing the upper bounds of component operational temperatures is conductive heat transfer from the rocket motor to the payload. To insure against this scenario, the payload and temperature-sensitive components will be thermally isolated from these heat sources.

6.2 Configuration Design

One of the key design issues for the STARSAT thermal system is thermal isolation of the components from excess conductive heat transfer. This will be accomplished by installing melamine foam at points of contact between the payload module and the fairing. This foam is highly resistant to both heat and cold, and also offers resistance to vibration and shear stresses at these contact points.

A rigid styrofoam modular enclosure will house STARSAT's battery and electrical system. The styrofoam will provide an effective layer of insulation for these components. A thin layer of cork will provide additional insulation. A multi-layer insulation (MLI) blanket will cover the cork. This material will reflect most of the heat lost by conduction back into the enclosure through the layers of insulation. The melamine foam installed at contact points between the payload and the rocket fairing will also help prevent conductive heat loss through the MLI blanket.

Components inside the enclosure will be thermally interfaced by means of a thermally conductive material. This will allow conduction of heat from some of the larger heat-emitting components to other components that need to be kept warmer. The objective of this method is to reach a near-thermal equilibrium state in which all the components are nearly the same temperature.

7. Command and Data Handling

The Command & Data Handling (C&DH) subsystem is required to handle ascent telemetry from STARSAT, and to identify, verify, and distribute commands to subsystems. The microprocessor and associated hardware must collect, format, multiplex, store, and download telemetry. The processor will need to perform orbital calculations, attitude determination and control calculations, health monitoring functions, and decode and issue commands.

7.1 Hardware Overview

The hardware objectives are to provide an efficient fault tolerant design, to provide ample processing power and storage capacity, to minimize power consumption and heat output, and to provide simple interfacing with external devices.

The subsystem design for STARSAT has utilized commercial off-the-shelf hardware almost entirely. The command and data handling system is composed of a PIC16C71 Micro-controller with standard memory and data bus structure. The PIC16C71 has a good reputation due to its reliability and its flexibility with different software packages and power control features.

The PICmicro programmable microcontroller (PIC16C71) acts as the payload CPU controlling the interface between the attitude determination system and its associated controls. In addition to ADCS, the PIC handles primary C&DH requirements such as: command (up-link) processing with 6.7 Kbps capacity, telemetry (down-link) processing with 8 Kbps capacity, and health monitoring; as well as, satisfying miscellaneous requirements such as the mission clock and watchdog timers. The PIC16C71 is a high-performance, low-cost, CMOS, fully static EPROM-based 8-bit microcontroller with on-chip Analog to Digital converter. It uses Harvard architecture and has only 35 single word instructions.

The command and data handling circuitry uses a National Semiconductor LMC6464 Operational Amplifier Integrated Circuit. This chip is a 14-pin integrated circuit, which contains a total of four on-board amplifiers. These amplifiers are wired to the gyroscope and GPS sensors for the purpose of boosting the voltage so the PIC processor can detect them.

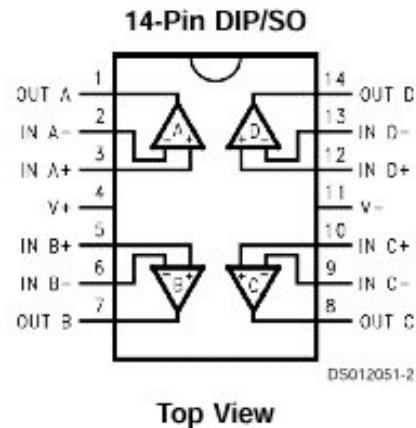


Figure 7.1: Op Amp chip layout

The circuitry also contains a SN5400, manufactured by National Semiconductor, a quad 2-input NAND logic gate. Only two of the four available NAND gates are used in this payload. The NAND logic gate is used to multiplex the GPS, Gyroscopic and PIC signals without causing the each other to short out. The output for this logic gate connects to the logic and input/output pins positive supply on the PIC. 10 volts directly from the battery, power the chip. Only NAND gate 1 and 2 are used. This implies pins 1 (A1), 2 (B1), 3 (Y1), 4 (A2), 5 (B2), 6 (Y2), are used for logic functions, while pin 14 (Vcc) uses an input voltage of 10 volts, and pin 7 (GND) is the ground lead.

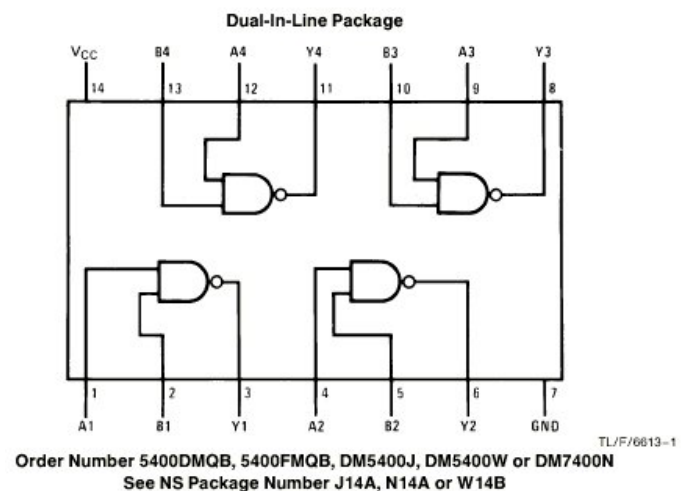


Figure 7.2: SN5400 Logic Gate

The TL082 integrated circuit, manufactured by Texas Instruments, is a dual JFET-input general-purpose operational amplifier. With respect to the payload, the TL082 takes the digital signals produced by the PIC and GPS and serves the purpose of unity-gain impedance matching. This means it allows the signal to be transmitted without current loss. This, in turn, readies it for input into the JRC4151D integrated circuit. The pin-outs for the TL082 are illustrated as follows:

TL082, TL082A, TL082B
D, JG, P, OR PW PACKAGE
(TOP VIEW)

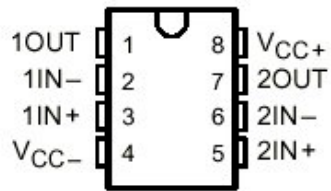


Figure 7.3: TL082 Integrated Circuit

Both on-board amplifiers are used. Input voltage for these amplifiers are 15 volts as converted from the battery by the 15-volt step-up converter. The signal input enters at 6 V when the NAND gate on the SN5400 is open, and 7.2 V when the gate is closed.

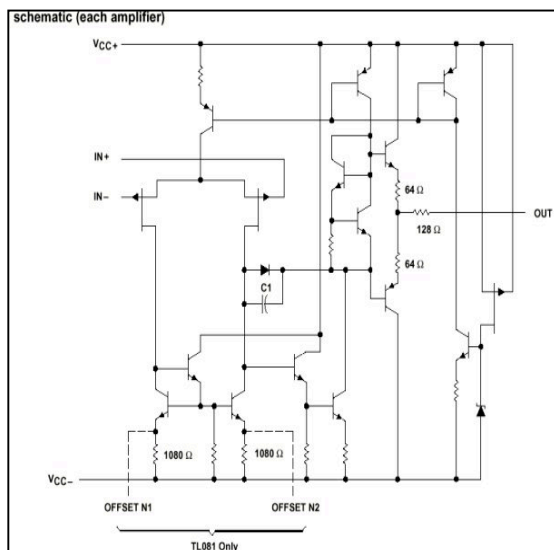
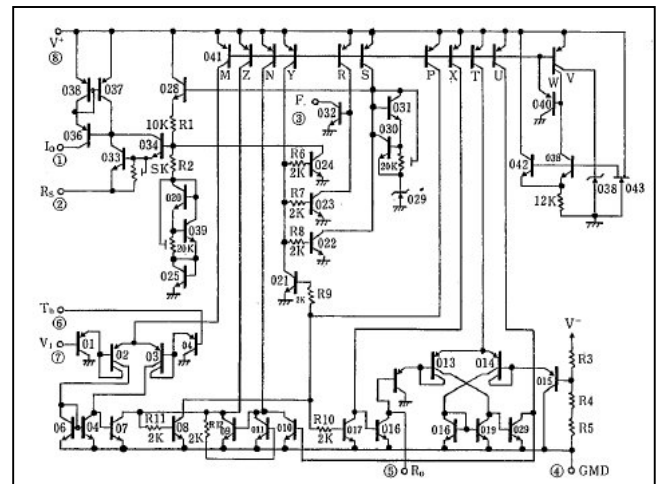


Figure 7.4: TL082 Circuit Schematic

The JRC4151D, manufactured by New Japan Radio Co., Ltd., serves as a voltage to frequency converter. The amplified GPS and PIC signals from the TL082 are converted from a digital signal into a frequency that the transmitter can then send to the receiver and ground station. A 15-volt input voltage converted from the 10-volt battery by the 15-volt step-down converter powers the chip. The 15-volt step-up converter converts the battery voltage from 10 volts to 15 volts. This voltage is desired for both the JRC4151D and TL082 integrated circuits. Additionally, the 5-volt step-down and 8 volt step-down converters use 15 volts as their input voltage. The 5-volt step-down converter takes the input voltage of 15 volts and outputs a smaller value of 5 volts. This value is favored by the measurement electronics, namely the gyroscope, operational amplifier, PIC16C71 microcontroller, SN5400 logic gate, and the GPS sensor. The circuit equivalent to the JRC4151D is as shown below:



The STARSAT ignition circuitry insures the satellite only fires at the designated inclination once at maximum altitude. The ignition circuit that will be used is a simple time delay switch utilizing discrete components. The variable resistor can be adjusted to provide an optimal time delay for the rocket platform to become stabilized before ignition. Once the transistor is triggered, the voltage will activate a relay to ignite the rocket motor. The PNP transistor is being used as a low voltage switch to activate the relay when the transistor conducts. The transistor will start to conduct when the base bias voltage reaches .707 volts. There is voltage applied to the base of the transistor through the electrolytic capacitor. The electrolytic capacitor will slowly charge with the rate based on the variable resistor utilizing the RC time constant concept. However, before the delay circuitry will even begin to charge all strategically aligned mercury switches must complete the circuit. This occurs only when the STARSAT vehicle is in proper orientation to initiate the launch trajectory. When the capacitor reaches .707 volts the transistor will conduct and energize the relay. The relay will then send the ignition voltage to the engine igniter.

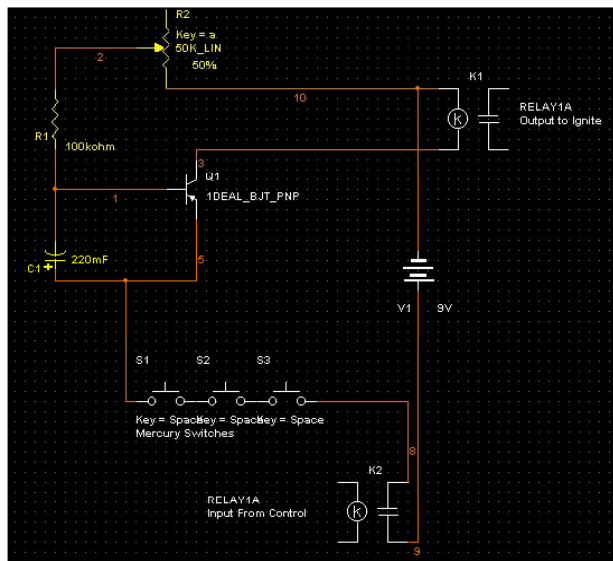


Figure 7.6: Ignition Circuit Schematic

The ignition sequence will be sent to the satellite as soon as the 20 km waypoint has been reached. Although the balloon will continue to rise the launch will occur as soon as the alignment is steady. Should the balloon reach bursting altitude without launch the deployment of the parachute is designed to prevent alignment of the switches at anytime and the completed assembly will return to earth for refurbishment and a second attempt.

7.2 Software Overview

The software objectives are to provide an efficient fault-tolerant design, to provide complete functionality for all spacecraft devices and to operate with a high margin of processing capability. In order to accomplish these objectives, the software design should have low level boot code located in ROM and high level boot and diagnostics located in EEPROM with an event driven scheduler loop allowing simple yet accurate sequence processing (Figure 7.7).

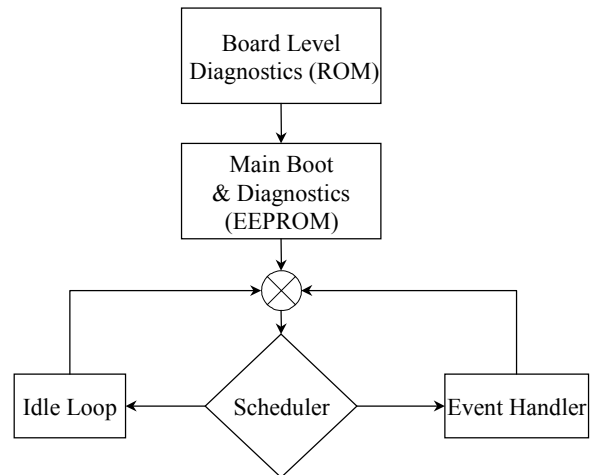


Figure 7.7: Software Block Diagram

8. Communications

The Telemetry, Tracking, and Command (TT&C) or Communications subsystem provides the interface between the launch system and ground station. The hardware and functions of this system pass attitude data and spacecraft payload data. Operator commands also pass through this subsystem to control the spacecraft and to operate the payload. The subsystem functions include: carrier tracking, telemetry, command reception and detection, ranging, and subsystem operations.

The STARSAT Communications system provides a hemispherical coverage for earth viewing and anti-earth viewing capable of simultaneous commanding and telemetry. Due to the unique nature of this initial payload, special meteorological frequency bands have been applied for use at Kennedy Space Center located at Cape Canaveral. The separate frequencies for commanding and telemetry coupled with the lower interference levels of the meteorological bands will provide the science team with high data quality.

The Communications architecture will process output data rates of 8 kbps and transmit them to the Earth during ascent. It will also pass incoming data rates to the Command and Data Handling subsystem at rates of 7 kbps.

8.1 UHF Uplink Receiver

A UHF command receiver with corresponding redundancy is capable of receiving digital commands with high reliability at any time and in any orientation. The two receivers shall be continuously powered on to eliminate switching that might present a possible single point failure. In addition to having no switches in the receive path, the communications system is built with redundant serial outputs to the C&DH to assure high fidelity. A high C/N (signal to noise) ratio has been designed to meet stringent bit error rates on the uplink in order to prevent misfire of the rocket motor.

Command rates of 1 MB/5 min. will more than satisfy the limited needs of this relatively autonomous launch vehicle. The associated C&DH subsystem has the capability of receiving asynchronous serial digital data at 7 kbps with a storage capability of over 1 MB.

The requested frequency for the command uplink is 405 MHz. A 30-foot Langley Space Center sponsored ground station will transmit data to the orbiting spacecraft from Cape Canaveral Airforce Station. A link analysis has been completed and is as follows for the uplink:

- 18 dB EIRP
- 2 dB losses
- 2 dB noise figure
- 0 dB reception gain
- 80 kHz bandwidth

On the spacecraft side, the receiver requires only 100mW of power. The dimensions are also a figure of merit in a small spacecraft such as STARSAT. The entire enclosure shall be but 50 X 65 X 25 mm and weigh just 200 g. The receiver can handle up to 14 KBPS using a GMSK modulation scheme.

8.2 VHF Downlink Transmitter

The Aerocomm 403 MHz transmitter is capable of transmitting real-time ascent telemetry at a rate of 8 Kbps during launch mode. The system will also transmit positional data during the Hohmann transfer maneuver. The telemetry subsystem will handle input serial digital data asynchronous from the C&DH system.

Utilizing a 403 MHz frequency range the VHF Transmitter will be capable of an 8 kHz bandwidth spread. Although only transmitting roughly .2 Watts the frequency bandwidth will enable sufficient data rates for transmitting the ascent data during launch. A 32 dB reception gain has been designed. The power consumption is reasonable for a low power transmitter requiring just 4 watts of input power.

A mass of 1.2 kg and dimensions of 180x95x45 mm make this the ideal transmitter for the STARSAT launch vehicle. The demodulator used is the relay between the receiver and the computer, which receives and records the information respectively. Since the transmitter on the satellite sends the information in two tones the computer is unable to read the data being sent. The data is sent into the ground station where it is converted into ones and zeros that a computer can read from a serial port. The FSK demodulator in the ground station takes the tones from the receiver and reproduces 5 volts and 0 volts for 1 and 0 respectively. However, since the computer can not read the 5 and 0 volts, the Aerocomm transceiver is used to take the voltage from the FSK demodulator and converts it to -12 volts for 1 and +12 volts for zeros. The Aerocomm is also capable of taking the data from the computer and converting back to the 0 and 5 volts, in order to program the GPS unit.

8.3 Antennae

Two UHF/VHF dual band antennae are mounted on either end of the spacecraft providing a hemispherical radiation pattern. These quarter-wave bent monopole antennae protrude from the launch tube allowing the science team to maximize the payload, while staying within structural restrictions. These antennae will also allow transmission during a variety of launch inclinations. The resulting system shall be capable of providing telemetry while in line of sight of the STARSAT ground station with the launch vehicle in any orientation. Linear polarization will be utilized despite a 3 dB loss due to the nature of the bent monopole. The signal to noise ratios however are still sufficient to meet the STARSAT telemetry requirements.

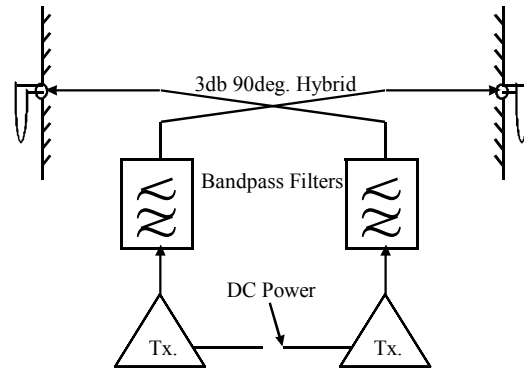


Figure 8.2 : Antennae Schematic
(2 of 4 Antennae Shown)

8.4 Communications Summary

System architecture diagrams have been finalized and the first revision of the printed circuit boards is complete. The STARSAT communications team is currently still working on the acquisition of requested frequencies.

A link budget has been completed detailing the flux density and carrier to noise levels for both the uplink and downlink. Utilizing an UHF/VHF link is a proven approach despite interference in the VHF regime.

9. Electrical Power Subsystem

The Electrical Power Subsystem team has designed the STARSAT launch vehicle with the ability to provide a continuous source of electrical power to all required loads for the duration of the mission.

The following are mission constraints and requirements for the design of the STARSAT power subsystem:

- Mission Type: LEO
- Mission Life: 1 day
- Vehicle requires a peak power of 10 W for transfer initiation and communication

9.1 Power Requirements

Payload power requirements are well suited for a small satellite design. The residual operating power of the spacecraft is 1 W. The peak load will be active only ten minutes during the ascent and ignition phase of the launch. This load will include the receiver, ignition circuitry, in addition to the passive mode electronics.

9.2 Power Source

There will be 1 ascent phase requiring a fully charged battery system for 10 minutes. Space Qualified 10-Volt batteries manufactured by VIZ were chosen for the STARSAT based on reliable radio sonde experience. The specifications for the batteries are given in Table 9.1.



Figure 9.1 : STARSAT Battery

9.3 Power Distribution

The general approach for the spacecraft's overall distribution system will be a decentralized, unregulated bus (Figure 11.1). Power converters will be installed at the various load interfaces to assure the required voltages are assigned.

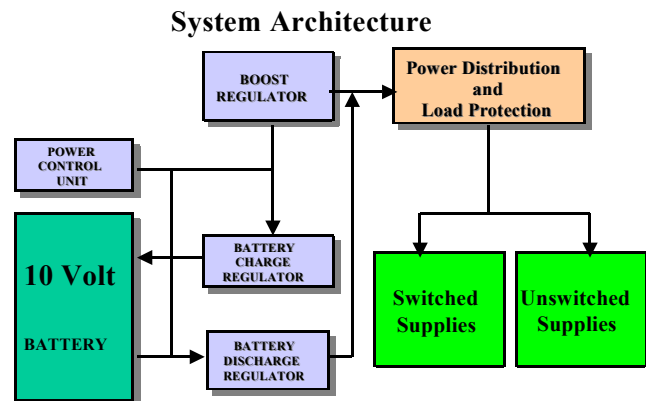


Figure 9.2 – Power Distribution Architecture

9.4 Power Regulation and Control

Each subsystem component requires a different operating voltage. Power converters will connect loads susceptible to noise or requiring voltage conversion to the distribution system. These converters isolate the load from the noise on the bus, and regulate the power provided to the load against disturbances. The typical power required by these two systems is estimated to be approximately 25% of the total power, 5% of which is lost in the transfer of power through the cables and the other 20% is power required to regulate each system.

10. Design Summary

The bus design is simple and uses COTS components for easy replacement and production. The vehicle is designed to be mass-produced to meet the growing needs of the small satellite market with reliability and quality.

A simple yet effective structural design has been implemented to maximize production capability and minimize launch risk. A flight proven rocket motor with optimized nozzle will carry small payloads into low earth orbit. MEMS microthrusters will provide efficient attitude adjustment during this ascent utilizing GPS and gyroscopic sensors. A robust command and data handling system will function with VHF/UHF communications to ignite and control the STARSAT launch. A space qualified 10-Volt battery will provide constant power to these subsystems while polyurethane foam controls bus temperatures. There are three phases from launch till the payload reaches orbit. During phase one, the balloon lifts the system from ground level up to the optimum height before the solid motor ignites. At phase two, the solid will fire and burn for a prescribed amount of time, ejecting the rocket from the launch tube and placing the module into a highly elliptical orbit. The module will fall past the earth, and upon reaching its perigee, phase three occurs. During phase three, an additional rocket motor assembly currently under design, will perform a Hohmann circularization, removing the module from its elliptical orbit. While in orbit, the MEMS thrusters can also perform small attitude corrections, and if necessary, minor orbital corrections.

Although the initial launch will not implement phase three, the new alternative system will ultimately provide a viable alternative to standard ground launched rockets to place payloads into a low-Earth orbit. By using less fuel, reducing the overall size, requiring fewer redundancy features, and utilizing a fuel that is both efficient and environmentally sound, the STARSAT balloon assisted insertion vehicle may be the next generation of orbital insertion.

STARSAT Summary

STARSAT 1 is expected to be completed July 20th and launch at soon after from a Naval vessel in the Gulf of Mexico. However, the system will still be ground validated at the Kennedy Space Center.

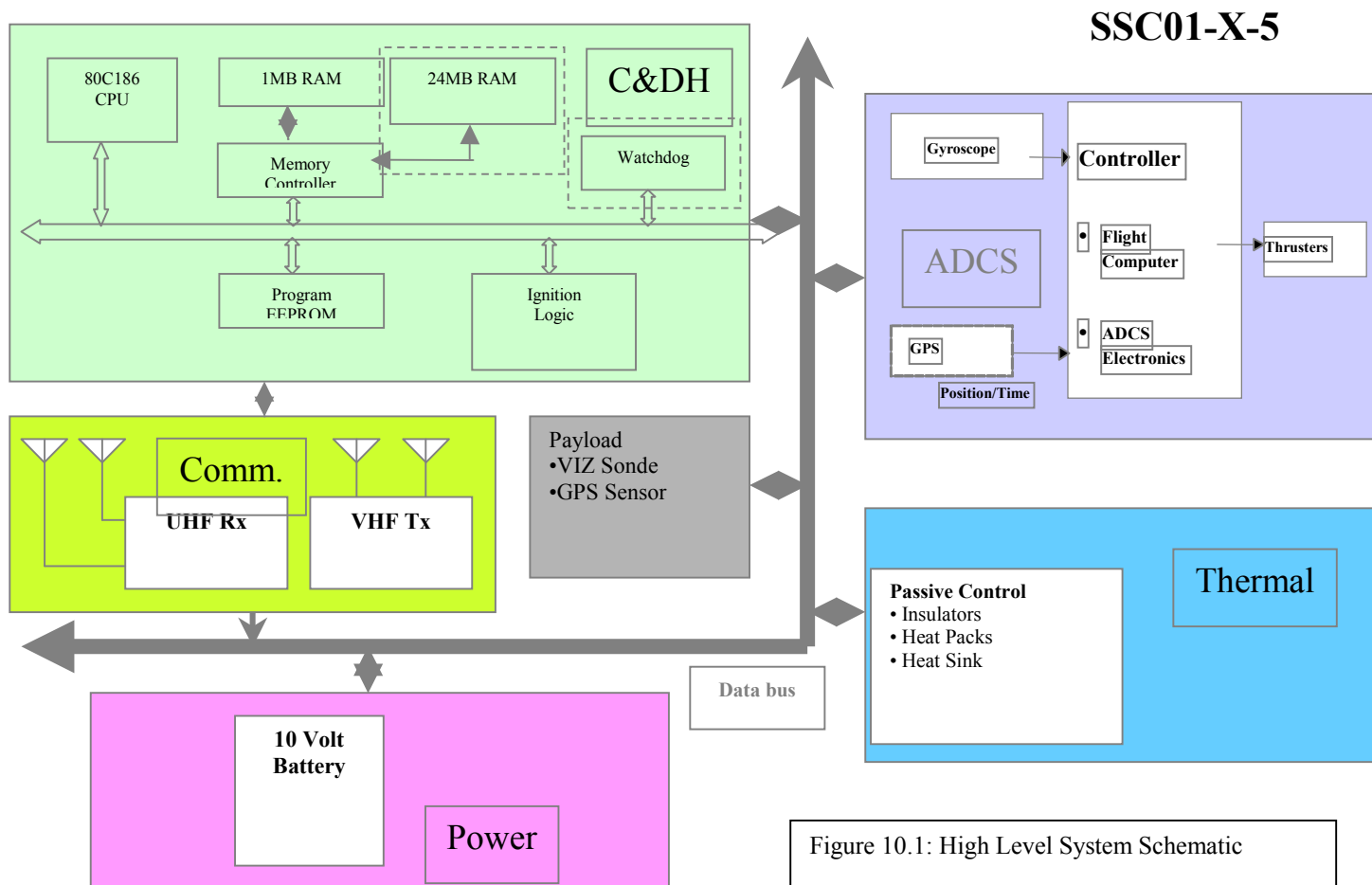
Phase one of the STARSAT launch system has been a resounding success. Engineering teams have turned concept into reality while management has secured funding and a customer base. The STARSAT lift vehicle is now ready to serve the small satellite needs of the future in a cost effective and environmentally conscious method.

Phase two of the project involves securing funding from either the government or capable third party to produce a final model from the prototype and begin rapid mass production. During this phase the overall reliability and quality of the design will increase dramatically as will the formality of the design specifications.

Phase three of the project will focus on identifying and meeting consumer needs and adapting the launch design to meet those requirements. More capable versions of the system will also developed and fabricated.

Acknowledgments

The STARSAT mission described in this report represents the work of a dedicated integrated project team at the Kennedy Space Center, including STARHUNTER CORPORATION, NASA, the University of Central Florida, the Florida Space Institute and other organizations. The authors are especially indebted to the engineers and management asked to sacrifice personal needs for the good of the program; as well as the contractors and supply partners who have designed and built this high quality space hardware. Our final acknowledgment goes to the entire STARHUNTER program for providing the leadership and vision to direct the worlds' future space development.



STARSAT DESIGN TEAM

• Mechanical Systems

- Lester Blandino :
Trajectory Calculation and Orbit Simulations
- Parker Lord :
Propulsion Design
- Eric Brown :
Nozzle Optimization
- Stephan Mancas :
Guidance Navigation and Control Systems
- Jen Lemanski :
Thermal Control Systems
- Bo Hutchinson :
Structural Design and Mechanical Control Systems

• Electrical Systems

- Eric Selvidge :
Space Electronic System Design
- Josko Zec :
Communications Systems
- Gerry Rivera :
Power System

Reference List

- Amsat. Doug Howard. 22 November 2000.
<http://www.amsat.org/amsat/balloons/balloon.htm>. 29 November 2000.
- Danny Banks. Homepage. 6 June 1999.
<http://www.dbanks.demon.co.uk/ueng/>. 23 November 2000.
- Larson, Wiley J. and Wertz, James R., ed. *Space Mission Analysis and Design, 3ed*. Torrance, California: Microcosm Press, 1999.
- NASA Jet Propulsion Laboratory. Robert H. Frisbee.
<http://sec353.jpl.nasa.gov/apc/Micro-propulsion/00.html>. 20 November 2000.
- The MEMS Exchangesm. 10 October 2000.
<http://www.mems-exchange.org/>. 22 November 2000.
- Hobbico Homepage
<http://www.hobbico.com/accys/hcam4000.html>